Himalayan Physics

Characterization of aerosol optical properties and their seasonal dynamics over Pokhara Valley, Central Nepal

https://doi.org/10.3126/hp.v14i1.85762

Shyam Prasad Kuikel[1*], **Santosh Pandey**[2]

1 Central Department of Physics, Tribhuvan University, Nepal

2 Prithvi Narayan Campus, Pokhara, Nepal

Abstract: Understanding the variation of aerosol optical properties is crucial for assessing air quality and climate impacts in mountainous regions such as Pokhara Valley, Nepal. This study investigates the monthly, seasonal, and wavelength-dependent behavior of aerosols over Pokhara during 2020-2022 using high-quality Level 2.0 AERONET data. Aerosol Optical Depth (AOD) at five wavelengths (440-1020 nm), together with the Angstrom exponent (α) and turbidity coefficient (β), was analyzed to characterize particle size and atmospheric loading. The results reveal pronounced seasonal variability, with the highest AOD during the pre-monsoon season (0.99 ± 0.12 at 440 nm in April) and the lowest during the monsoon (0.20 ± 0.05 at 1020 nm in August). A clear wavelength dependence is observed, with higher AOD at shorter wavelengths and lower values at longer wavelengths, indicating dominance of fine-mode aerosols. This seasonal contrast is governed by enhanced dust transport and biomass burning during the dry pre-monsoon months, while monsoonal precipitation efficiently scavenges aerosols. An inverse relationship between β and visibility demonstrates that increased aerosol loading degrades atmospheric clarity. Overall, the findings highlight the combined influence of seasonal meteorology, emission sources, precipitation-driven removal, and spectral aerosol behavior on air quality over Pokhara Valley, providing valuable insights for regional air-quality management, aerosol-climate studies, and health-protection strategies in Nepal's rapidly urbanizing mountainous environments.

Keywords: Aerosols • Seasonality • AERONET • Visibility

Recieved: 2025-10-27 **Revised: 2025-12-23** **Published: 2026-02-24**

I. Introduction

Air pollution remains one of the most critical environmental and public health challenges worldwide. Aerosols, which are minute solid or liquid particles suspended in the atmosphere, originate from both natural and anthropogenic sources. Natural processes, such as transboundary dust storms, while human-induced activities, such as traffic emissions, industrial combustion, and open burning, significantly

* *Corresponding Author: lekiuk777@gmail.com*

increase aerosol loading in Pokhara [1]. Once released, aerosols interact with atmospheric gases and radiation, thereby influencing weather, visibility, and climate [2]. Aerosol particles with diameters less than 2.5 μm can penetrate deep into the human respiratory system, leading to cardiovascular and pulmonary diseases. According to recent global assessments, long-term exposure to fine aerosols is associated with millions of premature deaths each year, making it one of the deadliest forms of air pollution [3]. Over the past two decades, satellite observations have revealed contrasting trends—while aerosol concentrations have decreased across North America and Europe due to stringent emission controls, South Asia continues to experience increasing levels [4].

Aerosols have different effects, such as scattering and absorption of solar radiation. Aerosols alter the amount of sunlight reaching the Earth's surface, reducing direct solar radiation, enhancing diffuse radiation, and modifying regional temperature gradients. These interactions affect atmospheric stability, cloud formation, and precipitation, making aerosols a vital component of the Earth's radiation balance and hydrological cycle [5, 6].

To quantify these interactions, researchers often rely on optical parameters such as Aerosol Optical Depth (AOD), the Angstrom exponent (α), and the turbidity coefficient (β). AOD (τ) measures the degree to which aerosols attenuate solar radiation in a vertical atmospheric column and serves as a primary indicator of aerosol loading. The Angstrom exponent (α), derived from the spectral dependence of AOD, provides information about the particle size distribution—higher values ($\alpha > 1$) indicate dominance of fine particles from combustion sources. In contrast, lower values ($\alpha < 1$) represent coarse particles such as mineral dust. The turbidity coefficient (β) quantifies atmospheric haziness and is directly related to visibility reduction. Together, these parameters allow the characterization of aerosol properties and their spatiotemporal variability [7, 8].

In Nepal, aerosol studies have gained increasing attention due to the country's complex topography and rapidly growing urbanization. Previous investigations have shown that aerosols over Pokhara are influenced by both local sources and regional transport of pollutants from the Indo-Gangetic Plain in different seasons [1]. Studies conducted in Pokhara have documented pronounced seasonal variations, with elevated aerosol loading during the pre-monsoon and winter months and reduced levels during the monsoon due to efficient wet scavenging [9].

Pokhara is in central Nepal within the Middle Hills region, but it lies immediately south of the High Himalayan range. The city is surrounded by major High Himalayan peaks, including the Annapurna and Machhapuchchhre, even though Pokhara itself is not in the High Himalaya. The city's basin-like topography and high humidity make it particularly sensitive to aerosol accumulation and dispersion. With an annual rainfall of approximately 3,900 - 4,800 mm, Pokhara is among the wettest urban areas in Nepal. Yet, recent climatological studies have revealed significant shifts: mean maximum and minimum temperatures have shown a consistent upward trend across most seasons. At the same time, total annual

precipitation has declined slightly, particularly during the monsoon and post-monsoon periods. Relative humidity frequently exceeds 75% during the monsoon season, creating persistently moist conditions that influence aerosol optical properties [10]. These evolving climatic patterns, combined with increased human activities and regional dust transport, make Pokhara an ideal location for studying aerosol dynamics in a complex mountainous environment.

Existing research on aerosol optical properties in Nepal has focused mainly on short-term observations or on major urban centers, leaving a significant knowledge gap regarding the wavelength-dependent behavior of aerosols in Pokhara Valley. Owing to its complex valley topography, substantial seasonal meteorological variability, and proximity to transboundary pollution sources, analysis of aerosol optical characteristics across multiple wavelengths, resolved at monthly and seasonal scales, remains limited. Moreover, most previous studies have primarily emphasized variations in Aerosol Optical Depth (AOD), while comparatively less attention has been given to atmospheric turbidity, visibility, and the classification of clean and turbid atmospheric conditions as a function of wavelength. Consequently, the combined assessment of AOD spectral dependence, turbidity, and visibility across different atmospheric regimes in the Pokhara Valley remains lacking.

Therefore, the present study aims to examine the monthly and seasonal variability of Aerosol Optical Depth (AOD) and its spectral dependence across multiple wavelengths (440 - 1020 nm) over Pokhara Valley during 2020 - 2022 using high-quality AERONET observations. Furthermore, it analyzes the relationships among AOD, turbidity, and visibility to evaluate changes in atmospheric visibility and distinguish between clean and turbid conditions across months and seasons. The outcomes of this study are expected to enhance understanding of aerosol-climate interactions in the Himalayan foothills, provide valuable insights for local and regional air-quality management, and contribute to the growing body of literature on aerosol optical behavior in South Asia's mountainous environments.

II. Methodology

This study utilized ground-based remote sensing data from the Aerosol Robotic Network (AERONET), a globally distributed network of automatic sun–sky radiometers established and maintained by the NASA Goddard Space Flight Center (https://aeronet.gsfc.nasa.gov). AERONET provides long-term, continuous, and readily accessible measurements of aerosol optical properties using standardized instrumentation and retrieval algorithms.

For this work, we employed data from the Pokhara Grande Hotel AERONET site (Birauta, Pokhara, Nepal; Latitude: 28.21°N, Longitude: 83.98°E; Elevation: ∼827 m a.s.l.), covering the period 2020 - 2022.The site is strategically located in the Himalayan foothills, making it well-suited to capture aerosol dynamics influenced by both local emissions and long-range transport.

The dataset comprised Level 2.0 (cloud-screened and quality-assured) observations processed using Version 3 algorithms. These data include key aerosol parameters such as Aerosol Optical Depth (AOD) at multiple wavelengths (440, 500, 675, 870, 1020 nm), Angstrom exponent (α), turbidity coefficient (β), and Precipitation (PW). Use of Level 2.0 ensures that retrievals are free from cloud contamination, calibration drifts, and major instrumental errors, thereby increasing confidence in subsequent analyses.

To investigate aerosol characteristics, the data were organized into daily, monthly, and seasonal averages. This approach enabled an assessment of short-term variability and seasonal patterns in aerosol loading. Statistical techniques were applied to examine interannual variability and to identify possible links between aerosol properties and regional meteorological conditions.

The relationship between AOD and angstrom exponent (α) is given by the power-law equation [11].

$$\tau = \beta\lambda^{-\alpha} \tag{1}$$

The wavelength in microns associated with AOD value is denoted by λ. Angstrom's turbidity coefficient is denoted by β.

Equation (1) can be written in the logarithmic format as:

$$\ln\tau(\lambda) = \ln\beta - \alpha\ln\lambda \tag{2}$$

Angstrom parameters (α and β) were obtained from equation (2). From the spectral AOD (λ), the angstrom exponent (AE) α can be further defined as:

$$\alpha = \frac{d\ln\tau\text{AOD }(\lambda)}{d\ln\lambda} = -\frac{\ln\left(\frac{\tau\text{AOD}(\text{at}\lambda_2)}{\tau\text{AOD}(\text{at}\lambda_1)}\right)}{\ln\left(\frac{\lambda_2}{\lambda_1}\right)} \tag{3}$$

where λ_1 and λ_2 represent two different wavelengths.

Atmospheric visibility (V in km) was estimated using the empirical relationship implemented by [9].

$$\beta = (0.5)\alpha \times \left(\frac{3.912}{V} - 0.01162\right) \times (0.02472(V-5) + 1.132) \tag{4}$$

where V denotes atmospheric visibility, which is inversely proportional to the aerosol extinction coefficient (b_{ext}) This formulation enables assessment of atmospheric visibility and classification of clean and turbid conditions based on aerosol optical behavior.

III. Results and Discussion

Spectral variation of aerosol optical depth (AOD)

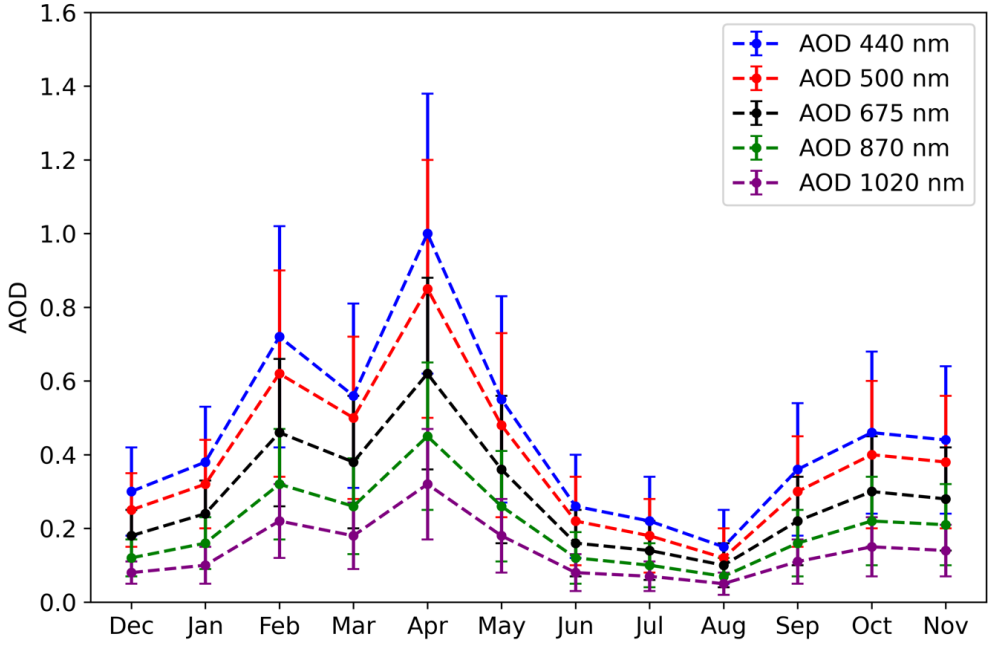

Figure 1. Monthly variation of aerosol optical depth (AOD) at multiple wavelengths (440-1020 nm) over Pokhara during the study period

Fig. 1 displays the monthly variation of Aerosol Optical Depth (AOD) at five wavelengths (440, 500, 675, 870, and 1020 nm) over Pokhara Valley during 2020 - 2022, a period strongly influenced by COVID-19 - related restrictions. The x-axis represents the calendar months from January to December, while the y-axis denotes the corresponding AOD values, which are dimensionless and indicate the magnitude of column-integrated aerosol loading in the atmosphere.

AOD values are consistently highest at shorter wavelengths (440 - 500 nm) and decrease toward longer wavelengths (870 - 1020 nm), indicating the dominance of fine-mode aerosols, which are typically associated with anthropogenic sources such as traffic, industry, and biomass burning [12]. During the monsoon months (June - August), AOD remains consistently low, with mean values of approximately 0.30 at 440 nm and 0.25 at 500 nm. This reduction is primarily attributed to intense monsoonal rainfall and high atmospheric moisture content, which promote efficient wet scavenging and washout of aerosols, thereby substantially lowering aerosol loading over the region. In addition, the elevated columnar water during the monsoon season enhances aerosol removal processes and suppresses aerosol accumulation, resulting in improved the visibility despite ongoing anthropogenic activities. A pronounced increase is observed from February to April, with a clear peak in April, where AOD reaches about 1.00 at 440

nm, 0.85 at 500 nm, and 0.62 at 675 nm. This springtime enhancement is attributed to a combination of regional biomass burning, dust transport, and gradual relaxation of mobility restrictions, leading to increased aerosol loading [13].

During these turbid periods, strong aerosol scattering and absorption reduce surface solar radiation and visibility, often producing a hazy atmosphere across the Pokhara basin. Similar pre-monsoon enhancements in AOD due to long-range dust transport and local emissions have been reported over other South Asian locations such as Lumbini, Kanpur, and Delhi [14]. The high AOD values and weaker wavelength dependence observed in this figure therefore indicate aerosol mixtures dominated by mineral dust with minor anthropogenic contributions, typical of pre-monsoon haze episodes in the central Himalayan foothills.

Following May, AOD values decrease sharply during the monsoon season (June - August). The lowest concentrations occur in August, with AOD dropping to approximately 0.20 (440 nm) and 0.15 (500 nm), reflecting the strong wet scavenging effect of precipitation, which efficiently removes atmospheric aerosols. Despite ongoing human activities, monsoon rainfall dominates aerosol removal during this period [15].

From September to November, AOD values show a secondary increase, with October values reaching around 0.46 at 440 nm and 0.40 at 500 nm. This post-monsoon rise is associated with reduced rainfall, resuspension of particles, biomass burning, and gradual recovery of economic activities as COVID-19 restrictions were further eased. The relatively lower AOD at longer wavelengths (e.g., ∼0.14 at 1020 nm in November) throughout the year suggests that coarse particles contribute less compared to fine aerosols.

Overall, the observed seasonal pattern–spring maximum, monsoon minimum, and post-monsoon recovery–is consistent with aerosol behavior over South Asian regions. However, the reduced wintertime and early-year AOD levels during 2020 - 2022 compared to typical climatological expectations indicate the impact of COVID-19 - related emission reductions, particularly on fine-mode aerosol concentrations.

Monthly relationship between turbidity coefficient (β) and visibility (Vis)

Fig. 2 illustrates the inverse relationship between the turbidity coefficient (β) and atmospheric visibility in Pokhara Valley from 2020 to 2022. The turbidity coefficient (red line) quantifies atmospheric haziness caused by aerosols, while blue line measures the visibility of the air. A clear seasonal pattern is evident–β peaks during the pre-monsoon months (March - May), when visibility simultaneously reaches its lowest values, and both parameters reverse during the monsoon season (June - September).

During the pre-monsoon period (March and April), elevated β values (up to 0.3) reflect intense aerosol loading and strong scattering of solar radiation, primarily due to increased dust transport from the Indo-Gangetic Plain, biomass burning, and local anthropogenic emissions [16]. These sources, combined with dry meteorological conditions and enhanced convective activity, lead to frequent haze episodes and

reduced atmospheric transparency. Consequently, visibility declines sharply to values often below 15 - 20 km. Such seasonal patterns have been widely reported across South Asia and the Himalayan foothills, where dry conditions enhance the suspension of coarse dust and anthropogenic aerosols [14, 17].

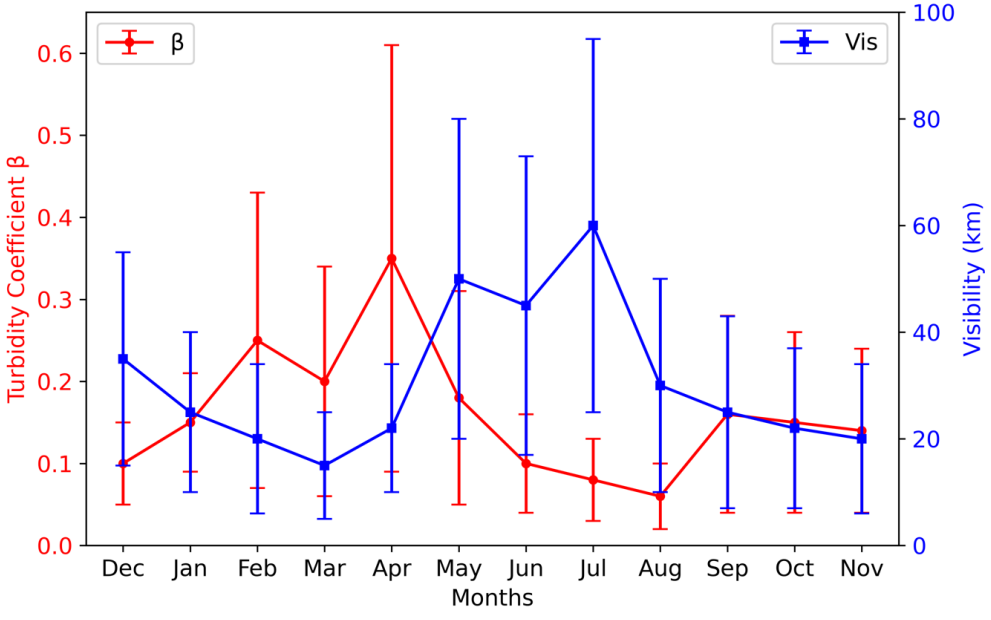

Figure 2. Seasonal variation of visibility and turbidity.

In contrast, the monsoon months (June - August) show a substantial decrease in β (≈ 0.05 - 0.1) and a significant improvement in visibility (> 60 km). This is attributed to wet scavenging processes, where raindrops efficiently remove suspended aerosols from the atmosphere. Heavy and persistent precipitation during this period effectively "cleanses" the air, leading to minimum turbidity and clearer skies [1].

The post-monsoon and winter seasons exhibit moderate β values (≈ 0.2 - 0.3) and variable visibility. During winter, fine-mode particles from combustion activities–such as domestic heating, traffic, and agricultural residue burning–accumulate under low wind speeds and stable atmospheric conditions, slightly increasing haze levels [13]. This explains the observed decline in visibility during December - January.

Overall, this figure demonstrates a clear opposite association between turbidity and visibility, confirming that aerosol concentration is the dominant factor controlling atmospheric visibility over Pokhara. These findings emphasize that aerosol variability is largely meteorologically driven, with monsoonal rainfall acting as a natural cleansing mechanism and dry-season transport and burning contributing to regional haze. Continuous monitoring of β - Vis relationships is therefore essential for understanding visibility degradation and guiding local air-quality management in the central Himalayas. Consistent with the present findings, previous studies have reported an opposite relationship between atmospheric turbidity and visibility, whereby increases in aerosol turbidity led to reduced visibility due to enhanced scattering

and absorption of solar radiation [9]. This inverse relationship reflects the fundamental role of aerosol loading and particle characteristics in controlling atmospheric transparency and supports the reliability of turbidity as an indicator of visibility degradation.

Monthly variation of aerosol optical depth and moisture-related parameters over Pokhara Valley

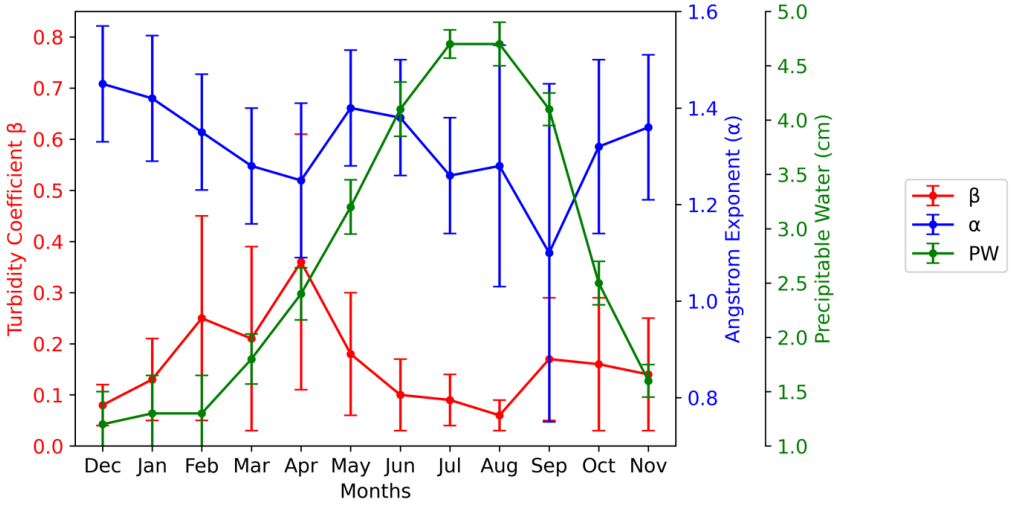

Figure 3. Monthly variation of turbidity coefficient (β), angstrom coefficient (α) and precipitable water (PW).

Fig. 3 illustrates the monthly variability of the Ångström exponent (α), turbidity coefficient (β), and precipitable water (PW) over the study period. The turbidity coefficient (β) represents the total atmospheric aerosol loading, while the Angstrom exponent (α) provides information on aerosol size distribution, with higher values indicating the dominance of fine-mode particles. Precipitable water (PW) reflects the total column water vapor and plays a key role in aerosol removal through wet scavenging.

During the winter and pre-monsoon months (December - April), β shows relatively elevated values, with a clear peak around February - April ($\beta \approx 0.25$ - 0.35). This increase suggests enhanced aerosol accumulation under dry conditions, weak dispersion, and limited precipitation, favoring the persistence o, f aerosols in the atmosphere. Concurrently, α remains relatively high (≈ 1.3 - 1.5) during this period, indicating a dominance of fine-mode aerosols, which are typically associated with anthropogenic emissions, biomass burning, and secondary aerosol formation. The relatively low PW values (< 2.5 cm) during these months further limit aerosol removal, allowing turbidity to increase. The relatively flat spectral curve (lower Angstrom exponent, $\alpha \approx 0.6$ - 1.6) further confirms the dominance of coarse dust particles over fine-mode aerosols. These conditions are also influenced by local open burning, vehicular emissions, and agricultural residue fires, which intensify in the pre-monsoon months, contributing both fine and coarse particles to the atmosphere [13].

With the onset of the monsoon season (June - August), PW increases sharply, reaching maximum values of approximately 4.5 - 5.0 cm, reflecting high precipitation. During this period, β decreases to its minimum values ($\approx$ 0.05 - 0.10), demonstrating the strong influence of wet scavenging processes that efficiently remove aerosols from the atmosphere. At the same time, α shows a moderate decline, suggesting changes in aerosol size distribution due to hygroscopic growth and preferential removal of fine particles. The effect of high rainfall leads to cleaner atmospheric conditions during the monsoon months. In the post-monsoon period (September - November), PW gradually decreases, while β shows remain constant. The inverse coupling between PW and β implies that aerosol concentration is strongly impacted by precipitation water, as high precipitation removal of particles from the atmosphere [18, 19]. The pattern reveal that Pokhara's atmospheric visibility and behavior are strongly controlled by monthly meteorology, emission intensity, and transboundary aerosol transport [13, 20].

Wavelength-dependent variation of aerosol optical depth (AOD) observed on clean days

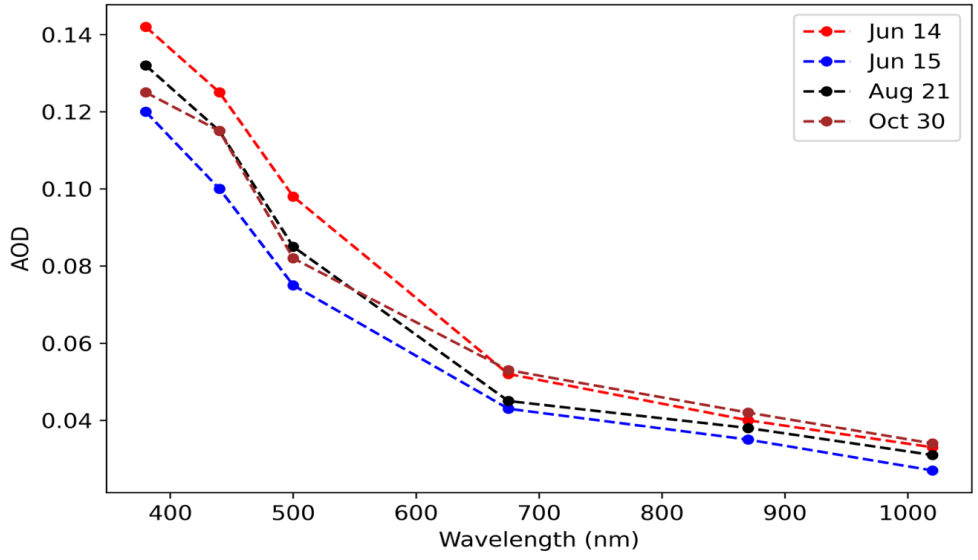

Figure 4. Wavelength-dependent AOD observed on four representative clean-sky days during the study period. Results illustrate the spectral dependence of aerosol loading under low-turbidity conditions.

The Fig. 4 illustrates the spectral variation of aerosol optical depth (AOD) as a function of wavelength for four selected clean-sky days (14 June, 15 June, 21 August, and 30 October). Clean days were identified based on low aerosol loading, characterized by AOD at 500 nm $\leq$ 0.15, turbidity coefficient (β) $\leq$ 0.15, and relatively high visibility ($>$ 30 - 40 km), indicating clear atmospheric conditions.

For all selected clean days, AOD shows a systematic decrease with increasing wavelength, with higher values at shorter wavelengths (380 - 440 nm; approximately 0.12 - 0.14) and substantially lower

values at longer wavelengths (870 - 1020 nm; approximately 0.03 - 0.04). This pronounced spectral dependence indicates the dominance of fine-mode aerosols, which preferentially scatter shorter-wavelength radiation under low aerosol loading conditions. The spectral pattern remains consistent across the four days, day-to-day variability in AOD. For example, 14 June exhibits slightly higher AOD values across most wavelengths, suggesting marginally enhanced aerosol presence, whereas 15 June represents the cleanest conditions, with the lowest AOD values throughout the spectrum. The cases from 21 August and 30 October fall between these extremes, reflecting moderate variability in aerosol concentration while maintaining similar spectral shapes. The persistence of a slight fine-mode particle even under clean conditions implies residual anthropogenic influence, possibly from local combustion sources and regional transport of fine aerosols [17, 21].

Overall, the similarity in spectral behavior across the selected clean days suggests comparable aerosol size distributions, while differences in AOD magnitude primarily reflect variations in aerosol loading rather than changes in particle type. The clear distinction between clean and turbid atmospheric conditions, based on quantitative thresholds of AOD, turbidity, and visibility, provides a robust framework for interpreting aerosol optical characteristics under contrasting atmospheric condition.

Wavelength-dependent variation of aerosol optical depth (AOD) observed on turbid days

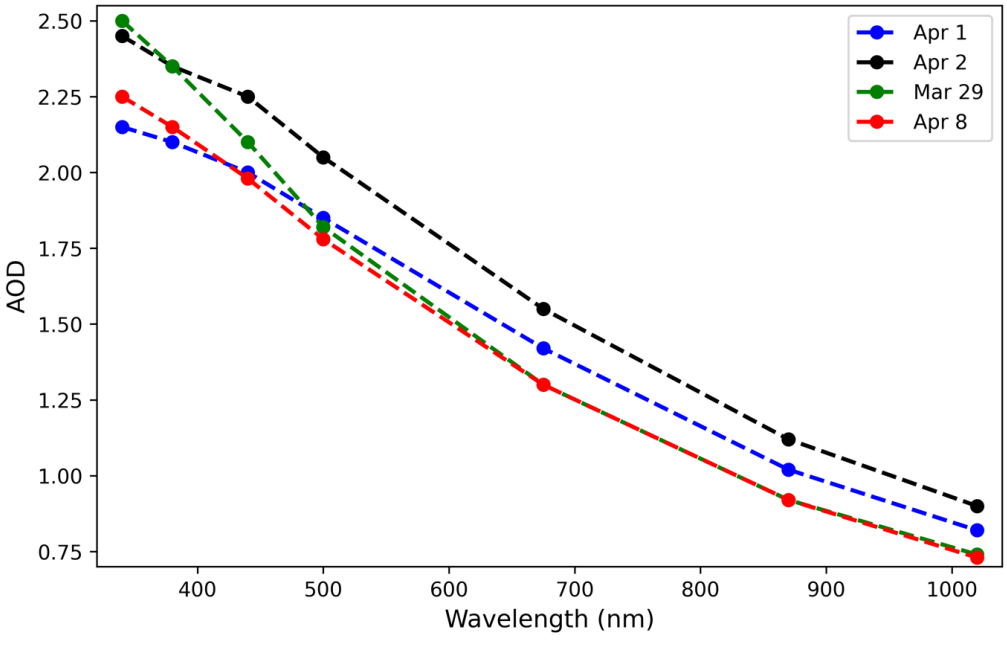

Figure 5. Wavelength-dependent AOD observed on four representative turbid days during the study period.

Fig. 5 illustrates the spectral variation of Aerosol Optical Depth (AOD) across multiple wavelengths (440 - 1020 nm) during turbid days in Pokhara Valley. AOD values are significantly higher (> 2.0 at 440 nm) compared to clean conditions, indicating severe aerosol loading and reduced atmospheric transparency. The AOD consistently decreases with increasing wavelength, though the slope is less steep than during clean days, suggesting a greater contribution from coarse-mode aerosols such as dust [13].

Overall, the figure demonstrates that turbid atmospheric conditions in Pokhara arise primarily from large, coarse-mode dust aerosols transported over long distances, enhanced by dry local emissions before the onset of the monsoon rains. These episodes have important implications for radiative forcing, visibility degradation, and air quality management in the region.

IV. Conclusions

This study provides a characterization of the monthly and seasonal spectral variability of aerosol optical properties over Pokhara Valley, Nepal, using AERONET Level 2.0 data from 2020 to 2022, a period that partially coincides with the COVID-19 pandemic. The results reveal that Pokhara's atmospheric environment is strongly influenced by both local and regional processes, with a clear annual cycle governed by meteorological conditions and emission patterns.

Aerosol Optical Depth (AOD) exhibited its highest values during the pre-monsoon season (March-May), reflecting intense aerosol loading dominated by coarse-mode particles originating from long-range dust transport and biomass burning activities. In contrast, the monsoon months showed a pronounced reduction in AOD due to wet scavenging, marking this period as the cleanest phase of the year. The winter season was characterized by fine-mode aerosols associated with local combustion sources under stable atmospheric conditions.

The Angstrom exponent (α) and turbidity coefficient (β) demonstrated complementary behavior, confirming that fine particles prevail in winter, whereas coarse dust dominates in pre-monsoon. The strong negative relation between turbidity and visibility, along with the positive relationship between precipitable water and Visibility conditions underscores the critical role of seasonal meteorology especially rainfall and humidity in regulating aerosol concentrations in the Himalayan foothills.

Spectral analyses further indicated that during clean days, the steep wavelength dependence of AOD corresponded to fine-mode anthropogenic aerosols, while during turbid days**,** a flatter spectral slope highlighted the influence of mineral dust and mixed coarse particles. These findings are consistent with previous studies conducted across the central Himalayas and the Indo-Gangetic Plain, confirming Pokhara's exposure to both local emissions and transboundary pollution transport.

The investigation demonstrates that Pokhara's aerosol characteristics are primarily shaped by seasonal meteorological dynamics, valley topography, and regional emission sources. Continuous monitoring

of aerosol optical properties is vital for improving air-quality forecasting, visibility management, and climate modeling in Nepal's mountainous regions. Future research integrating satellite observations, trajectory modeling, and chemical composition analysis would provide a more complete understanding of aerosol sources, transport pathways, and their long-term climatic impacts over the central Himalayas.

References

[1] Regmi J, Poudyal KN, Pokhrel A, Gyawali M, Tripathee L, Panday A, et al. Investigation of aerosol climatology and long-range transport of aerosols over Pokhara, Nepal. Atmosphere. 2020;11(8).

[2] Kommalapati RR, Valsaraj KT. Atmospheric aerosols and their importance. ACS Symposium Series. 2009;1005:1-10.

[3] Yang Y, Mou S, Wang H, Wang P, Li B, Liao H. Global source apportionment of aerosols into major emission regions and sectors over 1850–2017. Atmospheric Chemistry and Physics. 2024;24(11):6509-23.

[4] Hao H, Wang K, Zhao C, Wu G, Li J. Visibility-derived aerosol optical depth over global land from 1959 to 2021. Earth System Science Data. 2024;16(7):3233-60.

[5] Rapti AS. Atmospheric transparency, atmospheric turbidity and climatic parameters. Solar Energy. 2000;69(2):99-111.

[6] Utrillas MP, Martínez-Lozano JA, Cachorro VE, Tena F, Hernandez S. Comparison of aerosol optical thickness retrieval from spectroradiometer measurements and from two radiative transfer models. Solar Energy. 2000;68(2):197-205.

[7] Kokhanovsky AA. Remote sensing of atmospheric aerosol using spaceborne optical observations. Earth-Science Reviews. 2013;116:95-108.

[8] Khoshsima M, Bidokhti AA, Ahmadi-Givi F. Variations of aerosol optical depth and Angstrom parameters at a suburban location in Iran during 2009–2010. Journal of Earth System Science. 2014;123(1):187-99.

[9] Sapkota S, Gautam S, Pokhrel S, Gautam A, Basnet K, Mishra RK, et al. Study of aerosol optical properties in Lumbini, Nepal. BIBECHANA. 2023;20(1):1-9.

[10] Basnet K, Shrestha A, Joshi PC, Pokharel N. Analysis of Climate Change Trend in the Lower Kaski District of Nepal. Himalayan Journal of Applied Science and Engineering. 2020;1(1):11-22.

[11] Ångström A. Techniques of determining the turbidity of the atmosphere. Tellus. 1961;13(2):214-23.

[12] Sapkota S, Gautam S, Gautam A, Poudel R, Pokheral S, Basent K, et al. Comparison of aerosol optical properties over Lumbini, Pokhara and Langtang-Base Camp. Himalayan Physics. 2023:58-65.

[13] Ramachandran S, Rupakheti M. Inter-annual and seasonal variations in optical and physical characteristics of columnar aerosols over the Pokhara Valley in the Himalayan foothills. Atmospheric

Research. 2021;248:105254.

[14] Kumar S, Singh A, Srivastava AK, Sahu SK, Hooda RK, Dumka UC, et al. Long-term change in aerosol characteristics over Indo-Gangetic Basin: How significant is the impact of emerging anthropogenic activities? Urban Climate. 2021;38:100880.

[15] Sapkota S, Gautam S, Gautam A, Ale B. Correlative study of Aerosol Optical Depth with Precipitable Water over five AERONET stations across the world. BIBECHANA. 2023;20(3):213-23.

[16] Jha R, Adhikari B, Singh D. Study of aerosol optical properties at different tourist places of Nepal. BIBECHANA. 2021;18(1):170-83.

[17] Bhattarai BC, Burkhart JF, Stordal F, Xu CY. Aerosol optical depth over the Nepalese cryosphere derived from an empirical model. Frontiers in Earth Science. 2019;7:413408.

[18] Shrestha A, Subedi B, Shrestha B, Shrestha A, Maharjan A, Bhattarai PK, et al. Projected trends in hydro-climatic extremes in small-to-mid-sized watersheds in eastern Nepal based on CMIP6 outputs. Climate Dynamics. 2023;61(11–12):4991-5015.

[19] Thapa S, Pokhrel R, Banjara B, Nyaupane B, Dhakal A. Seasonal and topographical dynamics of precipitable water vapor in Nepal: A GNSS-based assessment. Dynamics of Atmospheres and Oceans. 2025;110:101548.

[20] Tripathee L, Kang S, Sharma CM, Rupakheti D, Paudyal R, Huang J, et al. Preliminary Health Risk Assessment of Potentially Toxic Metals in Surface Water of the Himalayan Rivers, Nepal. Bulletin of Environmental Contamination and Toxicology. 2016;97(6):855-62.

[21] Hegde P, Pant P, Naja M, Dumka UC, Sagar R. South Asian dust episode in June 2006: Aerosol observations in the central Himalayas. Geophysical Research Letters. 2007;34(23):L23802.